Available online at www.sciencedirect.com
ScienceDirect
Ceramics International 35 (2009) 821–825
CERAMICS INTERNATIONAL
www.elsevier.com/locate/ceramint

Aqueous processing of $Ce_{0.8}Sm_{0.2}O_{1.9}$ green tapes

Yen-Pei Fu *, Sih-Hong Chen

Department of Materials Science and Engineering, National Dong-Hwa University, Shou-Feng, Hualien 974, Taiwan

Received 18 December 2007; received in revised form 19 January 2008; accepted 24 February 2008
Available online 28 June 2008

Abstract

An aqueous tape casting of $Ce_{0.8}Sm_{0.2}O_{1.9}$ (SDC) ceramics was developed using poly(acrylic acid) (PAA) as dispersant, poly(vinyl alcohol) (PVA) as binder, poly(ethylene glycol) (PEG) as plasticizer, and deionized water as solvent. Surface properties of SDC powder with and without PAA dispersant were characterized by electrokinetic measurements. The rheology of the SDC slurries was evaluated with a rotary viscometer. The zeta potential measurement showed that the isoelectric point (IEP) for SDC powders in the absence of dispersant corresponds to a pH value of 3.66. The experimental results showed that the pH value greatly affects the rheology of the slurry. The optimum content to get a stable dispersed slurry is 2 wt% PAA in pH value range of 9–10. In presence of 2 wt% PAA dispersant, 55 wt% SDC powders exhibited shear thinning behavior, indicating that SDC slurry was homogenous and well stabilized. Homogeneous, smooth, and defect-free green tapes were successfully obtained by an appropriate slurry formula.

Keywords: Tape casting; D. CeO_2; E. Fuel cells

1. Introduction

Solid oxide fuel cells (SOFCs) are attracting widespread attention due to their high-energy conversion efficiency and low pollution. High-oxide ionic conducting solid electrolytes based on zirconia have been intensively investigated [1]. In order to reduce the operation temperature from 1000 to 800 °C or even lower, doped ceria has been considered as the solid electrolyte for moderate temperature solid oxide fuel cells [2]. In contrast to pure zirconia, $CeO_{2-\delta}$ has the fluorite structure with oxygen vacancies ($V_o^{\bullet\bullet}$) as the predominant ionic defects. The oxygen vacancy concentration and concomitant oxide ion conductivity, in CeO_2 can be increased by the substitution of a lower-valent metal such as Y [3], Sm [4,5], Gd [6,7], and Ca [8]. Pure stoichiometric CeO_2 ceramics are poor oxide ion conductors. However, the ion conductivity can be significantly improved by increasing the oxygen vacancies by the substitution of samarium, which is lower than 4+ in valence and upon substituting for Ce^{4+} are charge compensated by oxygen vacancies, for example:

$$Sm_2O_3 \xrightarrow{CeO_2} 2Sm'_{Ce} + 3O_o^x + V_o^{\bullet\bullet}$$

In general, decreasing the thickness of the electrolyte can further reduce the resistance to ionic transport and allows lower operating temperature of SOFCs [9]. Tape casting is mainly used to manufacture thin flat ceramic sheets. The thickness of tape cast products is typically 20 μm to a few millimeters. Typical applications include transducers, capacitors, pyroelectric infrared detectors and SOFCs [10]. Accordingly, in this study, we use tape casting to produce the electrolyte film of $Ce_{0.8}Sm_{0.2}O_{1.9}$ (SDC) for SOFC.

Traditionally, tape casting was done using organic solvents. Because of environmental, health, safety, and economic reasons, aqueous medium are substituting organic solvents [11]. Although, aqueous tape casting presented above-mentioned advantages, there are still several problems to overcome such as higher crack sensitivity, slow drying of the tape, flocculation and poor wetting of the slips [12,13]. The stability and rheological properties of ceramic suspension are influenced by many factors, such as pH, type and amount of dispersant and, the number of active groups on the powder surface. The stability and rheological properties of nanosized ceramics powders are more complex due to the particle interactions [14,15]. In this article, the rheological behavior of the slurries with addition of dispersant, binder, and plasticizer is studied. The stability of SDC suspension influenced by pH is also investigated.

* Corresponding author. Tel.: +886 3 863 4209; fax: +886 3 863 4200.
E-mail address: d887503@alumni.nthu.edu.tw (Y.-P. Fu).

0272-8842/$34.00
doi:10.1016/j.ceramint.2008.02.018

2. Experimental procedures

2.1. Starting materials

$Ce_{0.8}Sm_{0.2}O_{1.9}$ was synthesized by a coprecipitation method. The detailed procedure is described as follows: stoichiometric amounts of cerium nitrate hexahydrate ($Ce(NO_3)_3{\cdot}6H_2O$), and samarium nitrate hexahydrate ($Sm(NO_3)_3{\cdot}6H_2O$) were dissolved in distilled water. The final concentration of the stock solution was 0.2 M for Ce^{3+}. Then the ammonia (NH_4OH) solution was added to nitrates solution until pH 9.5, precipitates were formed. The resulting precipitate was vacuum-filtered, washed three times with water and ethanol, respectively. Then, the precipitate was dried at 80 °C in an oven. The coprecipitated hydrate powder decomposed to a polycrystalline oxide by heating to 600 °C for 2 h. The oxidation of Ce^{3+} to Ce^{4+} occurred during this stage. Deionized water was used as solvent. Poly(acrylic acid) (PAA) with molecular weight of 5000 g/mol was used as an electrosteric dispersant. Poly(ethylene glycol) (PEG) with molecular weight of 400 g/mol was used as plasticizer. Poly(vinyl alcohol) (PVA) with molecular weight of 13,000–18,000 g/mol was used as binder. All organic additives are soluble in deionized water. The content of organic components in this study was expressed in weight percent with respect to the SDC powder.

2.2. Zeta potential measurements

The zeta potential of suspension was measured using a Malvern Zetasizer nano-series. The suspensions were prepared by dispersing SDC powders (0.01 vol%) in deionized water. The pH value of suspension was adjusted by adding HNO_3 (0.1 M) or NH_4OH (1 M). The suspensions were mixed ultrasonically before the test to ensure that only the mobility of single particle was measured.

2.3. Rheological characteristic of slurry

Viscosity measurements were at room temperature performed using a rotary viscometer (Brookfield DV-II$^+$ Pro viscometer). SDC suspensions were prepared at solid loadings in the range of 50–60 wt% with 2 wt% PAA to determine the optimum amount of solid loading.

2.4. Slurry preparation and tape casting

The tape cast slurries were prepared in two stages. First, SDC powder and deionized water with optimum content of dispersant were mixed in a polyethylene jar with ZrO_2 balls for 18 h. Next, the binder and plasticizer solution were milled for 18 h to obtain good homogeneity. Subsequently, the slurry was vacuumed to deair. The optimum composition of slurry is given in Table 1. Tape casting was achieved using a laboratory-scale with a moving casting head on mylar substrate film. After tape casting, the tapes were left to dry at room temperature.

Table 1
Slurry formulation of aqueous tape casting SDC

Additive	Function	Content (wt%)
SDC	Ceramic powder	55
PAA	Dispersant	2
PVA	Binder	4.5
PEG	Plasticizer	4.5
Deionized water	Solvent	34

2.5. Characterization techniques

A computer-interfaced X-ray powder diffractometer (XRD; Model Rigaku D/Max-II, Tokyo, Japan) with Cu Kα radiation ($\lambda = 1.5418$ Å) was used to identify the crystalline phases. The particle size, morphology, and crystalline were determined by transmission electron microscopy (TEM; Model Jeol JEM-3010, Tokyo, Japan). Sample was prepared by ultrasonically dispersing the powders in ethanol, and then droplets were placed on carbon-coated Cu grids. The morphological features of the green tape were observed using a scanning electron microscope (SEM; Model Hitachi S-3500H, Tokyo, Japan).

3. Results and discussion

3.1. TEM observation

A TEM micrograph of $Ce_{0.8}Sm_{0.2}O_{1.9}$ nanopowders calcined at 600 °C for 2 h is shown in Fig. 1. The primary particle size is in the range of 40–50 nm. According to the selected area electron diffraction pattern, it revealed cubic phase. These particles are single crystal grains and exhibits high crystallinity, indicating a solid solution of SDC has been formed.

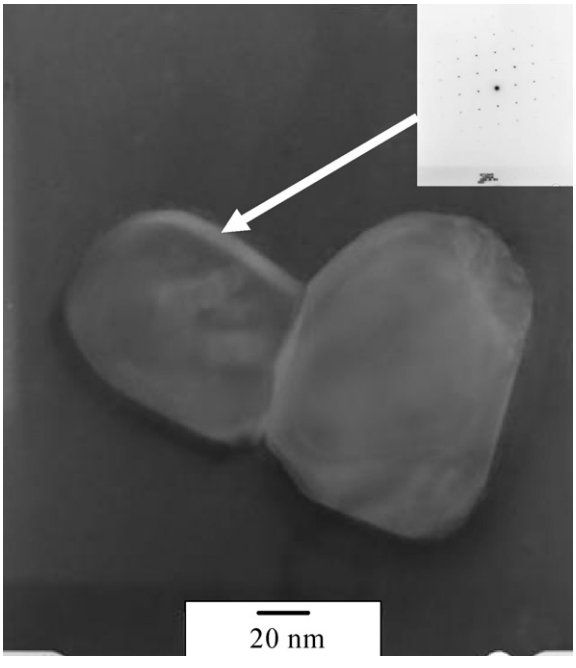

Fig. 1. Transmission electron microscopy micrograph of the SDC powders prepared from coprecipitation process and calcined at 600 °C for 2 h.

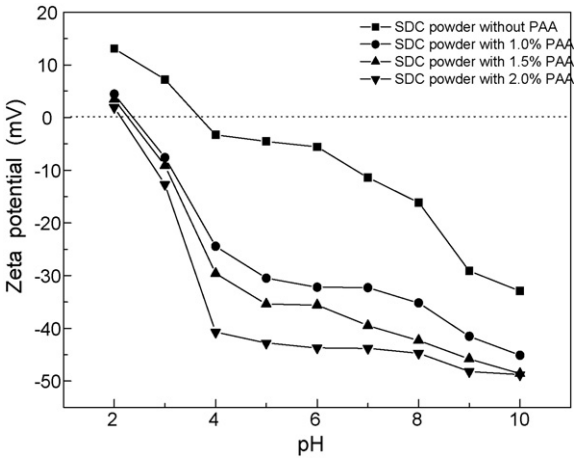

Fig. 2. Zeta potential of SDC powder as a function of pH at various amount of dispersant.

3.2. Suspension stability

Zeta potential measurements were performed to identify the optimum pH value and dispersant content for SDC suspension as shown in Fig. 2. Initially, there are a lot of positive charges on the surface of the powder, whereas when pH value is higher than isoelectric point (IEP) of the powder shows, there are a lot of negative charges on the surface of the powder. The IEP of SDC was about 3.66 in the absence of dispersant. The maximum zeta potential (absolute value) does not exceed 20 mV in the pH value range of 2–8, indicating that the electrostatic repulsion between SDC particles is insufficient for stabilizing suspension in the absence of dispersant. For the suspension containing 2.0 wt% PAA dispersant, the maximum zeta potential (absolute value) was about 48 mV at pH value of 10. It can be seen that the zeta potential (absolute value) was above 40 mV in the pH value range of 4–10. Therefore, we used a content of 2.0 wt% PAA for the tape casting slurry preparation. The result revealed that the zeta potential values (absolute value) increased with the dispersant amounts. Noticeably, the dispersant can significantly affect the zeta potential value. Moreover, the dispersant amount is greatly affected the interaction between SDC particles in aqueous suspensions. The function groups of PAA consist of carboxylic acid (COOH) groups, which can exist as COOH or dissociate to COO^-. The dissociation is written as follows:

$$A{-}COOH + H_2O \leftrightarrow A{-}COO^- + H_3O^+$$

Depending on the pH and ionic strength of the solvent, the fraction of function groups which are dissociated (COO^-) and those which are not dissociated (COOH) will change. Upon increasing the fraction dissociated, the electrical charge on the polymer changes from neutral to highly negative. As the pH increases, the extent of dissociation and negative charge of the polymer increase for PAA. Then as pH increases, a more negative charge adsorbs on the particles surface. It makes the zeta potential move negative.

According to the literature, metal ions on the surface oxide layer behave as Lewis acid [16]. In the presence of water, they may tend to coordinate H_2O molecules. Most oxide surfaces are hydrated, and a metal oxide, there will be MOH groups on the surface [17]. Below IEP, adsorption of H^+ ions leads a positively charged surface, whereas beyond IEP, adsorption of OH^- ions produces a negatively charged surface. Therefore, in this case, the dissociative chemisorption of water molecules led to an hydroxyl group on surface, which is known to specifically adsorb H^+ and OH^- according to the following equation [16]:

$$\equiv Ce - OH + H^+ \leftrightarrow \equiv Ce - OH_2{}^+, \quad K_1 = \frac{[Ce{-}OH^+]}{[\equiv Ce{-}OH][H^+]} \tag{1}$$

$$\equiv Ce - OH + OH^- \leftrightarrow \equiv Ce - O^- + H_2O, \quad K_2 = \frac{[Ce{-}O^-]}{[\equiv Ce{-}OH][OH^-]} \tag{2}$$

$$H_2O \leftrightarrow H^+ + OH^-, \qquad K_3 = [H^+][OH^-] \tag{3}$$

where K_3 is the equilibrium constant for the dissociation of H_2O, which is referred to as the ionic product of water. At the IEP, $[Ce{-}OH_2{}^+] = [Ce{-}O^-]$ so

$$[H^+]_{IEP} = \left(\frac{K_2 K_3}{K_1}\right)^{1/2} \tag{4}$$

Since pH is defined as $pH = -\log[H^+]$, the IEP of SDC can be written as:

$$pH_{IEP} = \frac{14 + \log K_1 - \log K_2}{2} \tag{5}$$

It is obviously, that pH_{IEP} depends on the values of K_1, K_2 and K_3, which are related to by the surface chemistry of the powder.

With $pH_{IEP} = 3.66$, is obtained from Eq. (5).

$$\frac{\log K_1 - \log K_2}{2} = -3.34$$

$$\frac{K_1}{K_2} = 10^{-6.68}$$

This indicates that K_2 much larger than K_1, implying that Eq. (2) dominates the reaction during the chemisorption process. This phenomena can be presumed that the surface $\equiv Ce{-}OH_2{}^+$ sites are withdrawn and create $\equiv Ce{-}O^-$ sites at

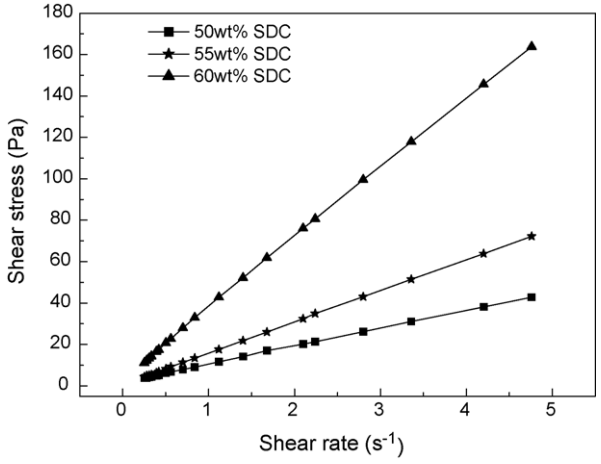

Fig. 3. Rheological curves of SDC slurries with 2 wt% PAA.

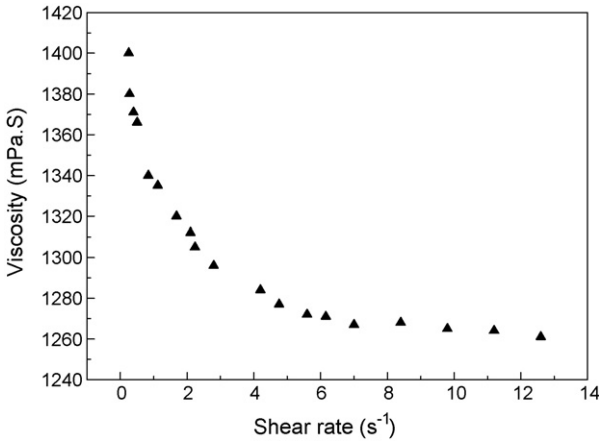

Fig. 4. Viscosity curves of suspensions containing with 55 wt% SDC powder and loading with 2 wt% PAA as a function of shear rate.

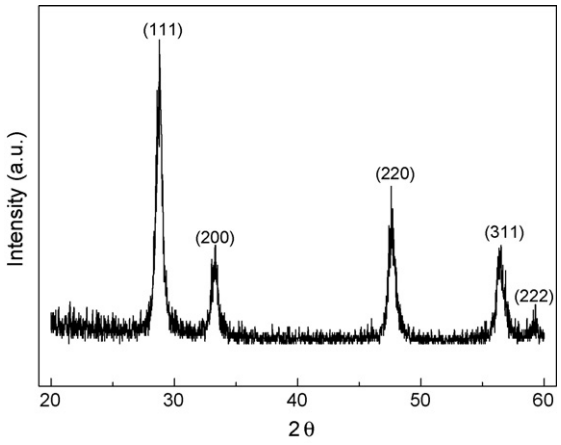

Fig. 5. XRD patterns for aqueous SDC green sheet.

equilibrium in water. According to the surface properties of CeO_2, polyelectrolyte PAA is selected as dispersant.

3.3. Properties of aqueous tape casting SDC slurries

According to zeta potential measurements, the dispersant amount of 2 wt% PAA was used for stabilization of slurry containing 50, 55, 60 wt% SDC powder with an adjusted pH of 9–10. Figs. 3 and 4 exhibit viscosity plots for SDC slurries at 50, 55, 60 wt% loading as a function of shear rate. The results reveal that the viscosity of slurries decrease versus increasing shear rates, typical of ''shear thinning'' behavior. This behavior is due to the attractive interaction of particles and the resultant formation of flocs in the slurry. Shear thinning fluid is favorable in slurry. Therefore, this fluid is preferred in tape casting because it reduces the mobility of constituents in the tape and preserves homogeneity of slurry [18]. All the slurries showed a shear thinning behavior with almost no time independence effect. The maximum viscosity corresponds to 60 wt% solid loading, this formula being too viscous to be used for tape casting. Contrarily, the slurry with 50 wt% solid loading showed the lowest viscosity, but was also unsuitable for tape casting. Accordingly, from experimental results, it was concluded that the optimum composition of slurry included, SDC powder 55 wt%, PAA 2 wt%, PVA 4.5 wt%, PEG 4.5 wt%, and deionized water 34 wt%.

The relationship between the viscosity and shear rate can be expressed by the Herschel Bulkley model [19]:

$$\eta = \frac{\tau_Y}{\dot{\gamma}} + K\dot{\gamma}^{n-1}$$

where τ_Y is the yield shear stress necessary to initiate flow, $\dot{\gamma}$ is the shear rate, K is the consistency index and n is the shear thinning constant [20]. For a Newtonian behavior, $n = 1$, for a dilatant behavior (shear thickening behavior), $n > 1$, and for a pseudoplastic behavior (shear thinning behavior), $n < 1.\tau_Y$, K and n determine according to this equation are 0.507, 1338.1, and 0.973 mPa, respectively. SDC slurry exhibited pseudoplastic behavior.

3.4. Characteristic of green tape

Fig. 5 reveals the X-ray diffraction patterns of aqueous $Ce_{0.8}Sm_{0.2}O_{1.90}$ green tape. The figure indicates that it contains only the cubic fluorite structure with space group *Fm*3*m*, no other crystalline phase is detected. All the peaks in the pattern match well with the Joint Committee of Powder Diffraction Standard (JCPDS) card file no. 34-0394. The microstructure of the green sheets of SDC is shown in Fig. 6. Both sides (top and

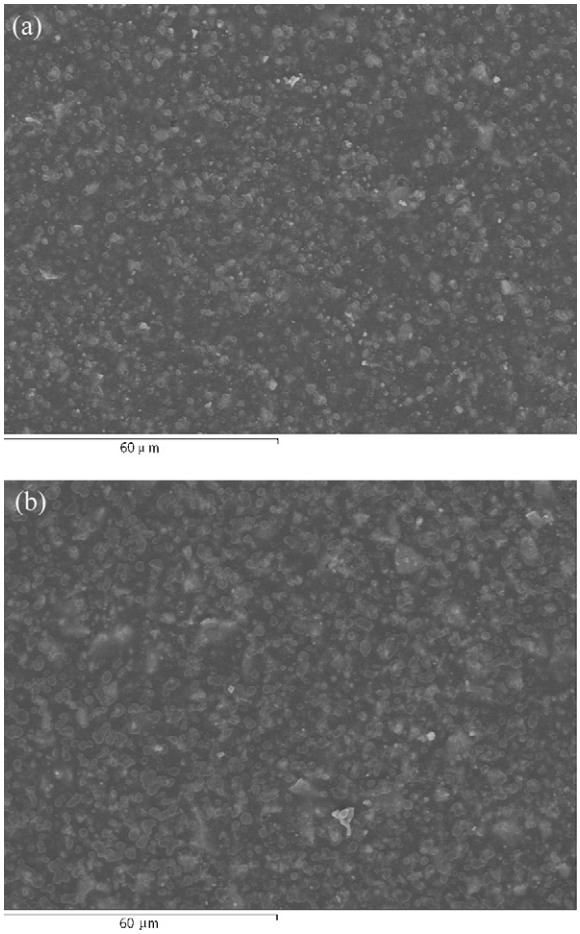

Fig. 6. SEM micrographs for dried tapes (a) top surface and (b) bottom surface.

bottom surface) of the tapes display very smooth surface. The homogeneity of the particle packing is ascribed to the fact that the SDC suspensions well dispersed.

4. Conclusions

In this study, using PAA as dispersant, PVA as binder, PEG as plasticizer, and deionized water as solvent, flexible and smooth SDC tapes have been successfully prepared by tape casting process. The zeta potential measurement revealed that IEP for SDC powders in the absence of dispersant was 3.66. In the presence of different dispersants in the range of 0.5–2 wt% of PAA, the IEP do not change obviously. For aqueous SDC suspensions, the pH value greatly affects the rheology of the slurries. Slurries containing 2 wt% PAA, 4.5 wt% PVA, 4.5 wt% PEG, and 55 wt% SDC powder exhibit shear thinning behavior, indicating that the slurry is homogenous and well stabilized. The homogeneous particle packing corresponds to the shear thinning behavior of the slurries. Both sides of the green tapes revealed smooth surfaces, no cracks were detected.

Acknowledgement

The author would like to thank the National Science Council of the Republic of China for financial support of this research under contract no. NSC 95-2221-E-259-023.

References

[1] B.C.H. Steele, Oxygen transport and exchange in oxide ceramics, J. Power Sources 49 (1994) 1–3.
[2] N.Q. Minh, Ceramic fuel cells, J. Am. Ceram. Soc. 76 (1993) 563–588.
[3] H. Yahiro, Y. Baba, K. Eguchi, H. Arai, High-temperature fuel cell with ceria–yttria solid electrolyte, J. Electrochem. Soc. 135 (1988) 2077–2080.
[4] T. Inoue, T. Setoguchi, K. Eguchi, H. Aria, Study of a solid-oxide fuel cell with a ceria-based solid electrolyte, Solid State Ionics 35 (1989) 285–291.
[5] C.C. Chen, M.M. Nasrallah, H.U. Anderson, Synthesis and characterization of $(CeO_2)_{0.8}(SmO_{1.5})_{0.2}$ thin films for polymeric precursors, J. Electrochem. Soc. 140 (1993) 3555–3560.
[6] H. Yahiro, K. Eguchi, H. Aria, Electrical properties and reproducibilities of ceria–rare-earth oxide systems and their application to solid oxide fuel cell, Solid State Ionics 36 (1989) 71–75.
[7] D.L. Maricle, T.E. Swarr, S. Karavolis, Enhanced ceria: a low temperature SOFC electrolyte, Solid State Ionics 52 (1992) 173–182.
[8] R.N. Blumenthal, F.S. Brugner, J.E. Garnier, The electrical conductivity of CaO-doped nonstoichiometric cerium dioxide from 700 to 1500 °C, J. Electrochem. Soc. 120 (1973) 1230–1237.
[9] J. Cheng, S. Zha, X. Fang, X. Liu, G. Meng, On the green density, sintering behavior and electrical property of tape cast $Ce_{0.9}Gd_{0.1}O_{1.95}$ electrolyte film, Mater. Res. Bull. 37 (2002) 2437–2446.
[10] A. Navarro, J.R. Alcock, R.W. Whatmore, Aqueous colloidal processing and green sheet properties of lead zirconate titanate (PZT) ceramics made by tape casting, J. Eur. Ceram. Soc. 24 (2004) 1073–1076.
[11] L.H. Luo, A.I.Y. Tok, F.Y.C. Boey, Aqueous tape casting of 10 mol%-Gd_2O_3-doped CeO_2 nano-particles, Mater. Sci. Eng. A 429 (2006) 266–271.
[12] T. Chartier, A. Bruneau, Aqueous tape casting of alumina substrates, J. Eur. Ceram. Soc. 12 (1993) 243–247.
[13] J.X. Zhang, D.L. Jiang, S.H. Tan, L.H. Gui, M.L. Ruan, Aqueous processing of titanium carbide green sheets, J. Am. Ceram. Soc. 84 (2001) 2537–2541.
[14] Y. Liu, L. Gao, Effect of 2-phosphonobutane-1,2,4-tricarboxylic acid adsorption on the stability and rheological properties of aqueous nano-sized 3-mol%-yttria-stabilized tetragonal-zirconia polycrystal suspensions, J. Am. Ceram. Soc. 87 (2003) 1106–1113.
[15] J.A. Lewis, Colloidal processing of ceramics, J. Am. Ceram. Soc. 83 (2000) 2341–2359.
[16] P.W. Schindler, Surface Complexes at Oxide–Water Interface, Ann Arbor Science Publishers, Ann Arbor, MI, 1981.
[17] M.N. Rahaman, Ceramic Processing and Sintering, Marcel Dekker, Inc., New York, 1995.
[18] X.J. Luo, B.L. Zhang, W.L. Li, H.R. Zhuang, Preparation of aluminum nitride green sheet by aqueous tape casting, Ceram. Int. 30 (2004) 2099–2103.
[19] J.S. Reed, Principles of Ceramics Processing., John Wiley, New York, 1995.
[20] J.H. Feng, F. Dogan, Aqueous processing and mechanical properties of PLZT green tapes, Mater. Sci. Eng. A 283 (2000) 56–64.